

Chain-Extended Polyethylene in Composites —Melting and Relaxation Behaviour—

N. A. J. M. VAN AERLE and P. J. LEMSTRA

*Department of Polymer Technology, Eindhoven University of Technology,
P. O. Box 513, 5600 MB Eindhoven, The Netherlands*

(Received August 27, 1987)

ABSTRACT: The melting and relaxation behaviour of chain-extended polyethylene/epoxy composites was studied. Using X-ray, DSC and birefringence techniques, it was shown that chain-extended ultra-high molecular weight polyethylene can be constrained fairly effectively by embedding in an epoxy resin, to prevent complete melting of the polyethylene far above the equilibrium melting point. Although the X-ray results look quite promising with respect to preservation of chain orientation in the fibres, both DSC and birefringence measurements indicate the presence of some relaxation/melting if the sample is heated above the orthorhombic to hexagonal transition point at 155°C. This solid-solid phase transition within the PE fibres is detrimental for the mechanical properties and consequently for the composite structure as a whole and sets an upper limit to the maximum use temperature.

KEY WORDS Polyethylene Tapes / Polyethylene Fibres / Composites /
Melting / Relaxation / WAXS / DSC / Birefringence / Hexagonal Phase /

The development of processes for the production of polyethylene (PE) fibres *via* melt spinning and subsequent drawing¹⁻³ as well as the introduction of the so-called gel spinning process, developed in the late seventies at DSM Research,⁴⁻⁶ made it possible to produce PE-fibres with excellent mechanical properties. Presently, the intrinsic possibilities of these fibres in textile and composite applications are explored in depth.⁷⁻¹²

Ultra-high molecular weight polyethylene (UHMW-PE) fibres, produced *via* gel spinning, exhibit favourable properties such as toughness, fatigue, chemical resistance and light resistance.⁶ A disadvantage of these PE-fibres is their low equilibrium melting point, which is reported to lie between 141.6 and 146°C.¹³⁻¹⁵ However, it is well known that *via* effective constraining the melting point can be raised. In this case the common orthorhombic crystal structure transforms into a hexagonal phase before final melting occurs. The occurrence of

a hexagonal structure in PE and similar paraffinoids with much lower molecular weight is known for a long time.¹⁶ The existence of the hexagonal structure as an intermediate between the common orthorhombic phase and the melt in PE was originally found by Clough.¹⁷ By using oriented cross-linked PE, constrained at constant length, an orthorhombic to hexagonal (o→h) phase transition could be observed at about 150°C. Since then more circumstances were noticed at which the o→h transition takes place in PE.¹⁸⁻³¹

By constraining oriented PE to a constant length, *i.e.*, *via* clamping the fibre/tape ends, the solid-solid o→h transition can be observed during temperature increase prior to melting.¹⁸⁻²³ Furthermore, it is well known that PE can exhibit an o→h transition prior to melting *via* another kind of constraining, *i.e.*, by heating the material under high hydrostatic pressures (>4 kbar).²⁴⁻³¹ In all cases the appearance of the hexagonal phase can be at-

tributed to strong restrictions, experienced by the molecules towards the adaption of a random coil conformation. These restrictions can be chemical cross-links, effective "entanglements" in very high molecular weight material, reduction of free volume under very high pressures or a combination of those factors.

The prime goal of the study presented here was to investigate whether the melting behaviour of chain-extended PE can be influenced by embedding in a matrix. An interesting question is, whether the composite matrix can prevent relaxation/melting of the PE fibres and/or tapes to such an extent as to preserve chain-extension, and hence the mechanical properties, by heating the composite above the equilibrium melting temperature of PE, which may occur for example in curing processes.

Using wide angle X-ray scattering, it will be shown that PE-fibres embedded in epoxy, exhibit an o→h transition prior to melting. The resulting hexagonal crystal structure will be compared with structures, induced *via* very high hydrostatic pressures. Additional results concerning the o→h transition obtained *via* differential scanning calorimetry and birefringence are discussed. Finally some results concerning the reversibility of the o→h transition are presented. This effect will be discussed in relation to the influence on mechanical properties of PE fibre reinforced composites.

EXPERIMENTAL

Materials

High-modulus tapes were prepared by drawing solution cast PE-films, obtained by dissolving 2 wt% UHMW-PE (Hostalen GUR-412, Hoechst/Ruhrchemie, $\bar{M}_w \sim 1700 \text{ kg mol}^{-1}$) in xylene at 130°C as described in literature before.³² The dried film was drawn manually at 120°C to a draw ratio of about 90 (the resulting Young's modulus was appr. 100 GPa). Ultra-drawn gel spun PE fibres were used, with a tensile strength and Young's modulus of

about 2.5 GPa and 115 GPa, respectively.

For all studies the fibres and tapes were subsequently washed with acetone and hexane, before embedding in an epoxy resin, Europox 730/XE 278 in a w/w ratio of 100/15. The curing of the resin was performed in 3 stages, *i.e.*, 30 min at room temperature, followed by 1 and 2 h at 80 and 120°C, respectively. No specific surface treatments were applied to improve the fibre-matrix adhesion.

Techniques

The wide angle X-ray scattering (WAXS) studies were performed using a Statton camera, equipped with a temperature controlled cell. The accuracy of the temperature ranged within 1 to 2°C. This was checked using adipic acid ($T_m = 153^\circ\text{C}$) for temperature calibration.

Ni-filtered Cu- K_α -radiation was generated at 50 kV and 35 mA and the X-ray exposure time was usually chosen to be 30 min. The sample to film distance amounted 50 mm, in some cases 30 mm.

Melting endotherms were determined using a Perkin-Elmer DSC-2 calorimeter. A standard heating and cooling rate of 10°C/min was adopted. Indium was used for temperature calibration ($T_m = 156.6^\circ\text{C}$). The temperatures at the maximum of the endotherms were taken as the transition temperatures.

High temperature birefringence measurements were performed, using a Zeiss polarizing microscope fitted with a Mettler FP-2 temperature regulated hot-stage. The birefringence was measured using a quartz rotary Berek compensator. For these studies the epoxy embedded PE fibres were kept between two glass slides in order to improve thermal contact. Before each measurement the sample was kept at least 5 min at the required temperature. The birefringence was calculated from:

$$\Delta n = \phi/d_t$$

where Δn is the birefringence, ϕ the measured optical retardation at the centre of the fibre

and d_f the fibre diameter.

RESULTS AND DISCUSSION

Melting Behaviour

Oriented UHMW-PE Tapes. A drawn PE tape with a final width and thickness of about 2 mm and 15 μm , respectively, and a Young's modulus of appr. 100 GPa at room temperature was embedded in an epoxy resin. The WAXS patterns presented in Figure 1 were recorded as a function of temperature, with the primary beam directed perpendicular to the tape surface. The presence of the epoxy matrix gives rise to a strong amorphous halo in the WAXS pattern.

At room temperature, the WAXS patterns of the tape exhibit characteristics pointing to the presence of biaxial orientation, *i.e.*, intense

(110), very weak (200), and relatively intense (020) equatorial reflection spots.^{32,33}

Upon heating a weak signal, attributed to the presence of a small fraction PE in the hexagonal phase, can be detected at 152°C superimposed on the common orthorhombic phase. Further heating leads to the complete disappearance of the orthorhombic characteristics at 155°C. The constraining effect, caused by the embedding epoxy system is effective enough to prevent relaxation and subsequent melting of the PE tape up to temperatures of about 155°C. By varying the X-ray exposure time a lifetime of the hexagonal structure in these uncrosslinked tapes of about 30 min at 155°C was deduced. The thermal stability of the system studied is rather poor compared to constrained *crosslinked* PE tapes described in literature,^{17,19,22,23} indicating that crosslinking increases the stability in constrained oriented PE samples. In order to compare the constraining efficiency of epoxy for PE-tapes and fibres, the melting behaviour of embedded fibres will be discussed in detail in the following sections.

Oriented UHMW-PE Fibres. Figure 2 shows a temperature series of WAXS patterns of embedded PE fibres. The detected circular reflections arise from the aluminum foil in which the sample was wrapped to ensure good heat conduction. Just as in the case of the PE tape, the presence of the epoxy can be observed from the amorphous halo in the WAXS patterns. Unfortunately this halo coincides with the amorphous halo of PE. It is therefore quite difficult to observe changes in amorphous material (molten PE fraction) during heating cycles.

Upon heating a weak reflection, assigned to the (100)_h (hexagonal (100)) reflection of PE, appears very close to the (110)_o (orthorhombic (110)) reflection at a temperature of 150°C. This (100)_h reflection becomes increasingly intense at the expense of the (110)_o and (200)_o reflections, within a temperature range of about 3°C. Although there is a small increase

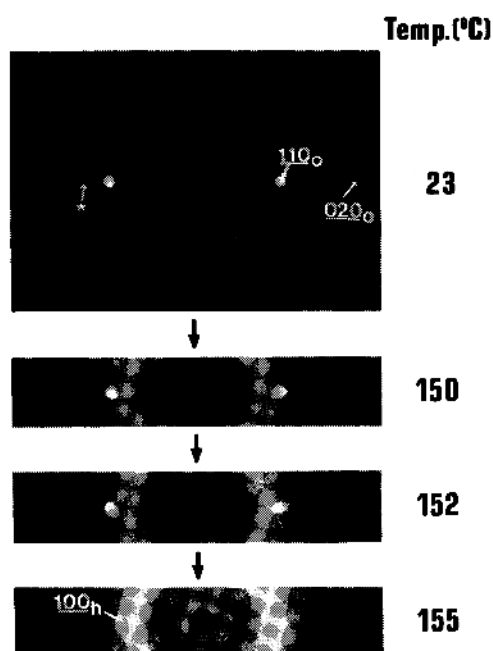


Figure 1. Series of WAXS patterns as a function of temperature for an epoxy embedded PE-tape ($\lambda=90$). The tape was mounted with the drawing direction vertical and the tape surface perpendicular to the incident beam. * indicates the PE (110)_o and (200)_o reflections due to Fe- K_α -radiation, arising from Fe impurity in the Cu-tube.

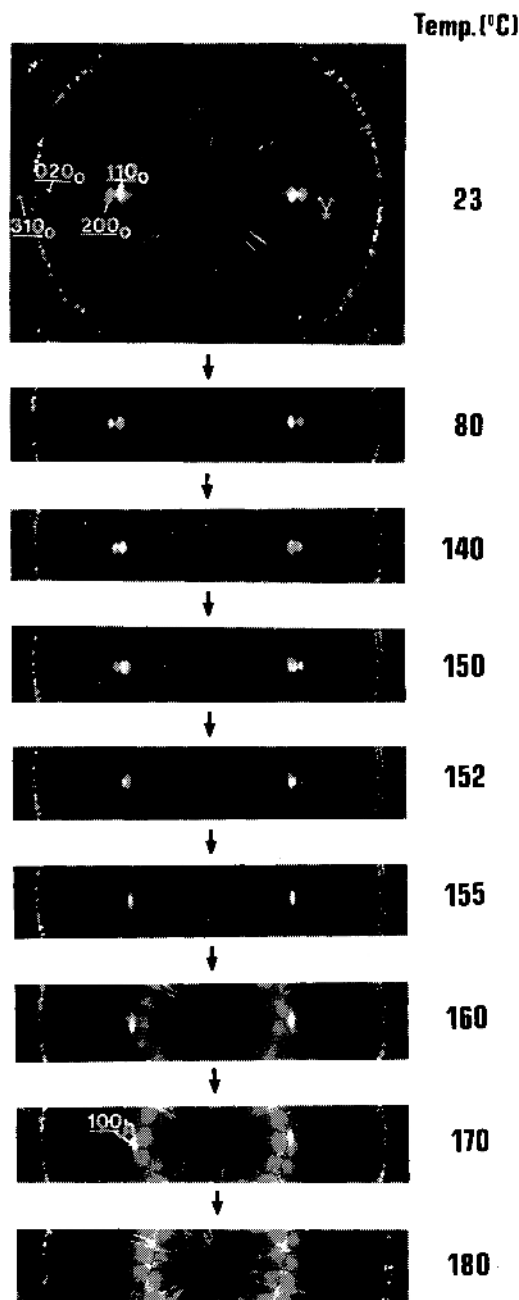


Figure 2. Series of WAXS patterns of epoxy embedded PE-fibres as a function of temperature. The outer reflection ring and streaks originate from the used Aluminum coating. * indicate PE-reflections caused by Fe- K_{α} -radiation.

in the hexagonal reflection arc, the $(100)_h$ reflection shows the same orientation characteristics as the $(110)_o$ and $(200)_o$, implying that no drastic orientational changes occur during the $o \rightarrow h$ transition. The simultaneous existence of both phases at temperatures between 150 and 153°C seems to present an equilibrium situation, since there is no detectable intensity change of any reflection if the samples are kept within this temperature range for at least 2 h. At 153°C all orthorhombic characteristics have disappeared. Further temperature increase leads to the disappearance of the hexagonal crystal phase at temperatures above 175°C. The absence of any PE-reflection above this temperature points to the presence of completely molten PE.

Additional information about temperature effects on the crystal structure of both the orthorhombic and hexagonal phase was obtained by studying the changes in the lattice spacings. In Figure 3 the results are presented for the equatorial $(110)_o$, $(200)_o$, $(020)_o$, $(310)_o$, and $(100)_h$ reflections. Starting at room temperature a gradual increase in spacing is found for all reflections with increasing temperature. Upon heating the spacing of the $(110)_o$, $(200)_o$, and $(310)_o$ increases by 1.6, 4.8, and 3.9%, respectively whereas the spacing of the $(020)_o$ reflection increases by less than 0.4%. Similar results were reported in the past.³⁴⁻³⁸ They indicate an anisotropic thermal expansion in the orthorhombic plane normal to the polymer chains, in which nearly all the expansion occurs in the a -axis direction. This anisotropy can be understood in terms of differences in binding forces between the PE-chains along the a -axis and b -axis. Since the distance between two parallel chain segments is smaller along the b -axis, the binding forces along the b -axis will be higher. This results in an energetically favourable a -axis expansion.

Despite the gradual change, the $o \rightarrow h$ transition is still discontinuous. From Figure 3 it can be inferred that the increase in lattice spacing is highest for the equatorial $(100)_h$

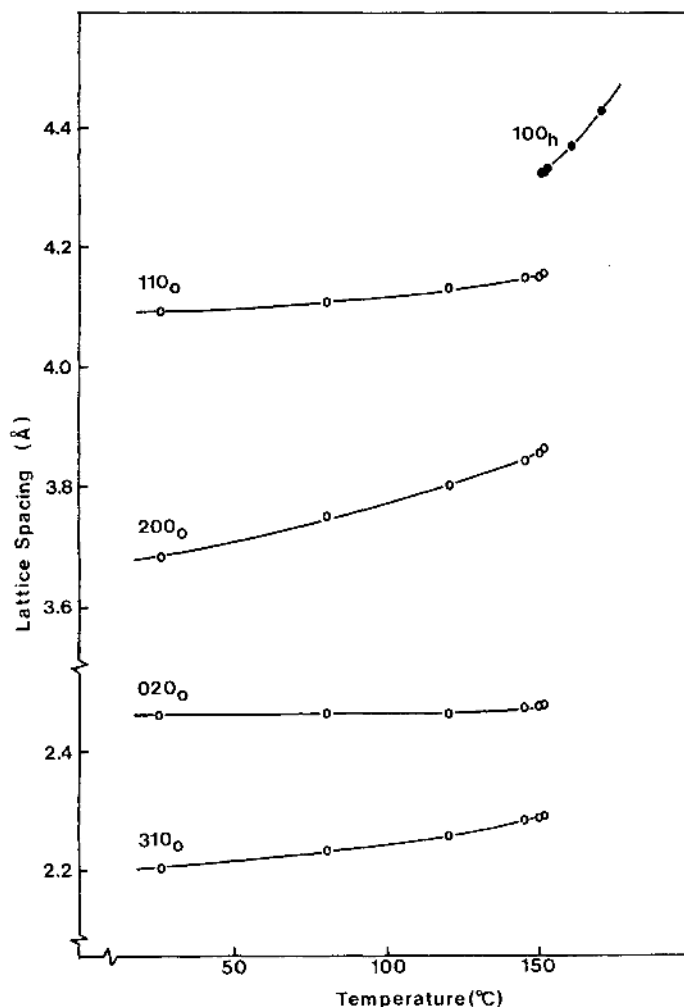


Figure 3. Influence of temperature on several PE lattice spacings of epoxy embedded PE-fibres.

reflection. As was pointed out in the past for oriented PE materials,^{18,21,22} this implies the presence of an increased molecular chain mobility in the hexagonal phase.

More information about the hexagonal crystal structure was obtained *via* WAXS experiments, varying the sample to film distance (in order to increase the detectable 2θ -region) and the exposure time. To avoid disturbing aluminum reflections, the epoxy embedded PE-fibres were not wrapped in aluminum foil this time. In Figure 4 two characteristic WAXS patterns are shown, recorded at appr.

155°C, together with a schematical drawing. As can be seen, one strong and two rather weak equatorial reflections can be discerned. The corresponding lattice spacings of 4.34, 2.50, and 2.18 Å agree very well with the (100)_h, (110)_h, and (200)_h reflections respectively, as reported in literature. There is no detectable reflection except on the equator, even after a very long exposure time only diffuse scattering with some orientation at the meridian can be detected, indicating relatively large conformational disorder of the molecules along the *c*-axis direction. The distance from

the equator of $0.43 \pm 0.01 \text{ \AA}^{-1}$ corresponds to a fibre period of $2.31 \pm 0.05 \text{ \AA}$. Similar results were obtained for oriented PE-fibres in which the hexagonal phase was induced and kept under high pressures and temperatures

($> 8 \text{ kbar}$, $> 260^\circ\text{C}$).^{29,39,40} The results imply that the hexagonal phases, either induced *via* heating constrained fibres at atmospheric pressures or at very high hydrostatic pressures, show similar X-ray characteristics and hence

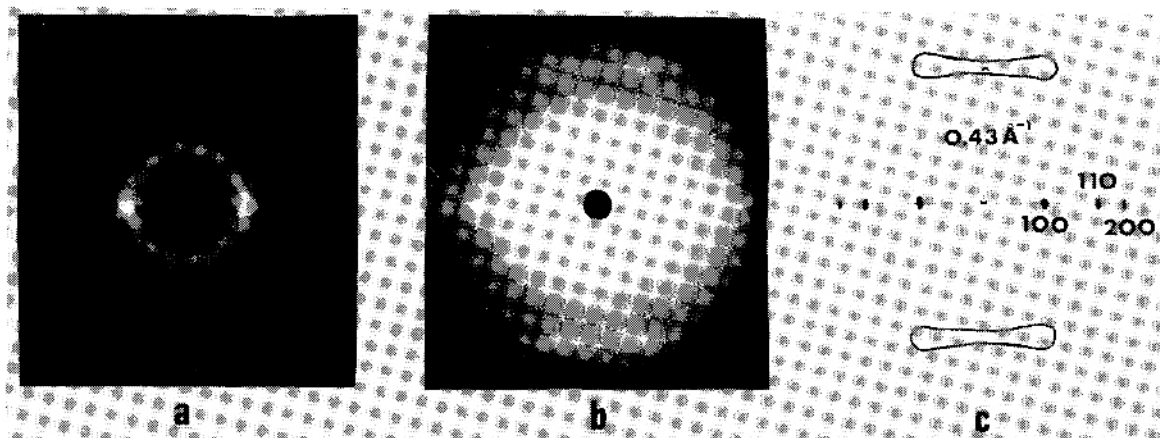


Figure 4. WAXS-patterns of epoxy embedded PE-fibres at 155°C : (a) exposure time of 30 min; (b) exposure time of 5 h; (c) schematic picture obtained from (a) and (b).

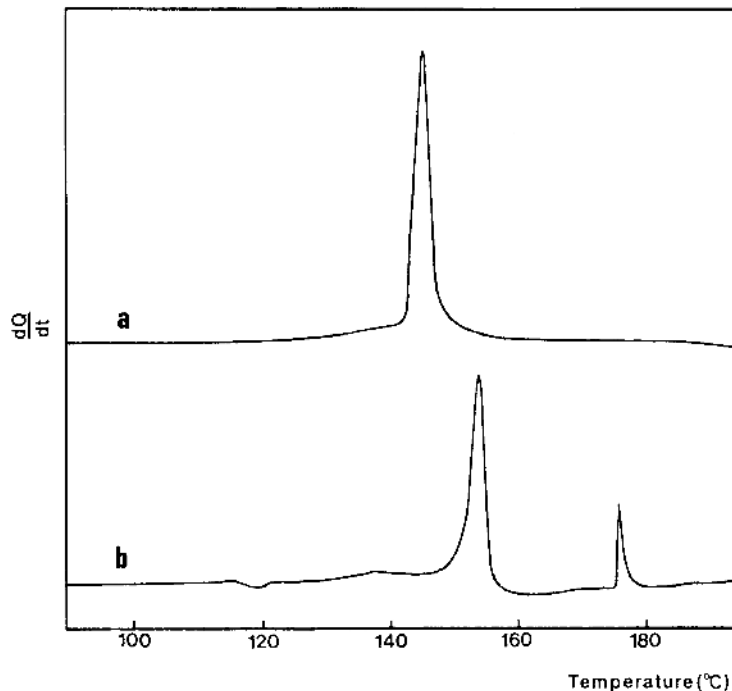


Figure 5. Comparison of DSC melting endotherms of (a) unconstrained and (b) epoxy embedded PE-fibres, heating rate $10^\circ\text{C min}^{-1}$.

similar crystal structures.

Compared to the results for embedded tapes, see former section, the obvious conclusion is that fibres can be constrained more effectively than tapes, *e.g.*, epoxy embedded fibres can be kept at temperatures up to 170°C for at least 5 h before the sample is completely molten whereas tapes melt at 155°C within less than 1 h.

Differential Scanning Calorimetry (DSC)

To investigate the *o*→*h* transition in more detail, additional experiments by means of DSC were performed. In Figure 5 the DSC curves of unconstrained (5a) and constrained (5b) fibres are compared.

The former DSC curves was obtained by heating chopped fibres (appr. 2 mm in length) in a droplet of silicon oil to obtain optimum heat conduction and avoid constraining effects. These unconstrained fibres exhibit an endothermic maximum at 145°C which is common for highly chain-extended PE.^{6,41} The constrained fibres on the other hand, show two endothermics with corresponding transition temperatures of 153°C and 176°C, respectively. Compared to the WAXS data described

earlier, we may ascribe the first endotherm to the *o*→*h* transition. The second endotherm however, reflects a more or less abrupt relaxation of the chain-extended molecules, resulting in melting of the hexagonal phase. This relaxation effect may be caused by a sudden loss of constraining properties of the embedding material, as can be inferred from the anomalous shape of the melting curve and from optical microscopy.

Birefringence

The temperature dependence of the birefringence of PE-fibres embedded in an epoxy resin was studied. As can be observed in Figure 6 the small initial increase in birefringence up to about 140°C is followed by a small decrease. At $151 \pm 1^\circ\text{C}$ a drastic decrease can be noticed whilst the fibres exhibit complete loss of fibrillar inhomogeneities, present in the original fibres. This latter effect is clearly observable *via* a polarizing microscope. Further heating results in a continuous decrease in birefringence and at about $172 \pm 5^\circ\text{C}$ stress regions become visible in the epoxy material surrounding the fibres.

Comparing the DSC and X-ray results, the

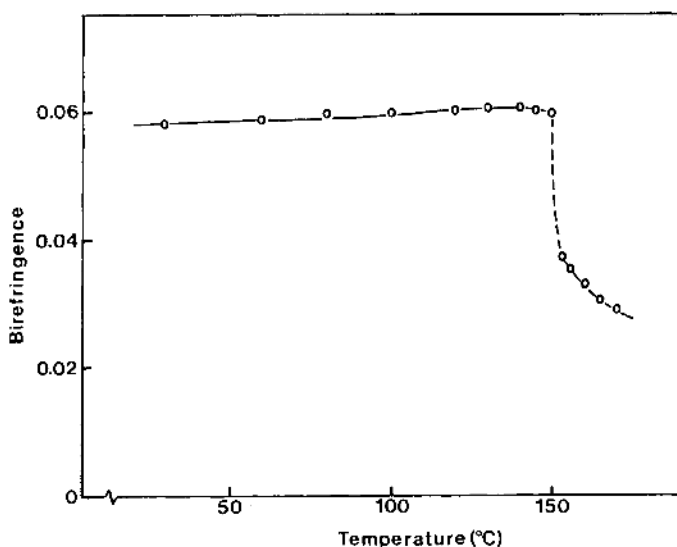


Figure 6. Influence of temperature on the birefringence of an epoxy embedded PE-fibre.

first drastic decrease in birefringence at about 151°C can be ascribed to the o→h transition, suggesting that the hexagonal structure of oriented PE is less birefringent. Similar results were found for constrained cross-linked PE

tapes, drawn 40 times.⁴²

Relaxation and Reversibility

All results discussed up to now definitely prove the existence of an o→h transition in oriented PE materials, constrained in a composite matrix. Especially for the use of PE fibres in fibre-reinforced composites, it is important to know the effect of heating above this o→h transition upon the properties of the composite in view of curing cycles and maximum use temperatures. To get a better insight in possible structural changes occurring during and above the o→h transition, reversibility studies were performed.

X-Ray Studies

Figure 7 shows some WAXS patterns, recorded for epoxy embedded PE-fibres during a heating and subsequent cooling series. At 140°C the common orthorhombic structure is present. Heating to 150°C indicates the transformation of some orthorhombic PE into hexagonal material. The transition is completed at 153°C. To study the reversibility of the o→h transition, the sample was subsequently cooled. At 150°C some hexagonal PE has re-transformed into orthorhombic PE. Close quantitative inspection of the recorded patterns reveals some super-cooling during the h→o transition. Analogous results

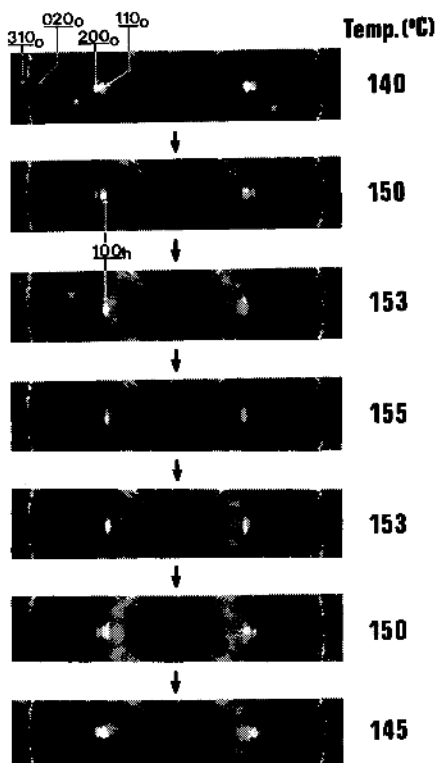


Figure 7. WAXS patterns of epoxy embedded PE-fibres at various temperatures.

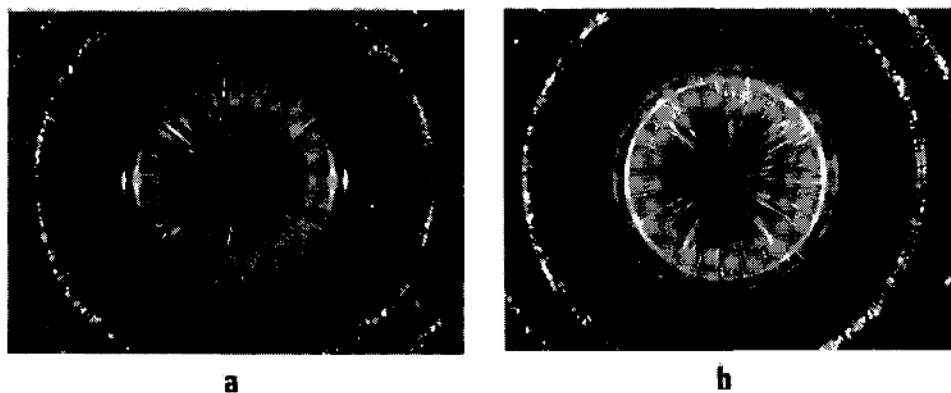


Figure 8. WAXS patterns of epoxy embedded PE-fibres at room temperature, after keeping the composite at 170°C (a) or 180°C (b) for 1 h.

were observed using constrained, oriented, cross-linked PE.^{21,43} Comparing the WAXS pattern of the composite at 140°C (before further heating) and 145°C (after cooling down from 155°C) reveals no detectable decrease in orientation, despite the fact that the embedded fibres were kept in the rather mobile hexagonal phase for at least 2 h. Unfortunately, due to the epoxy scattering halo, it was impossible to observe possible changes in amorphous PE material *via* X-ray. However, if the composite is heated up to temperatures above 170°C for more than 2 h, much orientation appears to be lost after cooling down as can be seen in Figure 8a. Surprisingly, however, if the PE fibres are kept in the molten state (at 180°C) for about 1 h, the WAXS pattern still reveals some preferential orientation after cooling down to room temperature (Figure 8b). This suggests that it takes more than 1 h before molten, epoxy embedded, UHMW-PE fibres become com-

pletely isotropic. The combination of the high viscosity of molten UHMW-PE and the constraining properties of the resin reduces the rate of the process, responsible for relaxing oriented material into the isotropic state.

Since the WAXS technique is not adequate to differentiate between chain-orientation and chain-extension, additional DSC and birefringence measurements were performed in order to elucidate possible relaxation effects.

Differential Scanning Calorimetry

Some results obtained from reversibility studies by means of a DSC are shown in Figure 9. The first heating scan (curve a) shows one distinct endotherm with a corresponding transition maximum at 154°C, assigned to the o→h transition. Cooling the sample results in the detection of two exotherms at 121 and 146°C respectively (curve b). As is known from literature the exotherm at 121°C is caused by crystallization of relaxed,

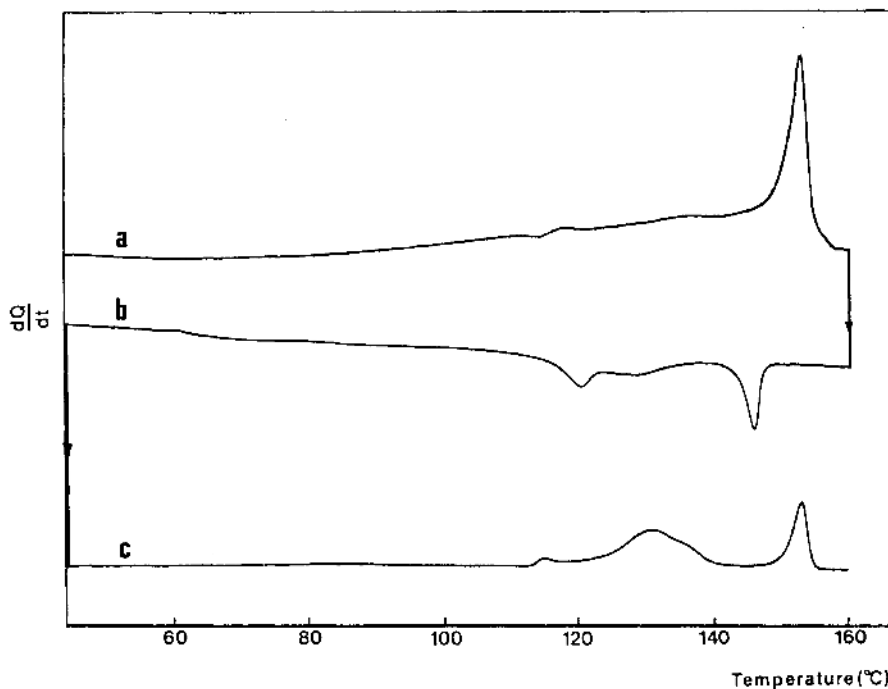


Figure 9. Series of DSC curves of epoxy embedded PE-fibres: (a) first heating scan; (b) cooling scan; (c) second heating scan.

molten material whereas the latter exotherm (146°C) arises from the h→o transition. These assignments are supported by the DSC curves, observed during a second heating scan (curve c), which reveals two endotherms. The temperatures of 131 and 154°C correspond to the melting of isotropic PE and the o→h transition of chain-extended material, respectively.

The DSC curves can be explained straightforwardly. During the first heating scan the orthorhombic chain-extended PE transforms into the hexagonal structure at 154°C. Since the molecular mobility in this latter phase is relatively high, stress relaxation takes place, resulting in partial melting of relaxed PE chains, whilst unrelaxed chains remain in the hexagonal crystal structure. The combined presence of molten and chain extended crystalline material explains the observed cooling and second heating DSC curves.

Birefringence

Finally the reversibility of the o→h transition was investigated *via* birefringence studies. The results, observed *via* heating epoxy embedded PE fibres are already discussed in a former section. A drastic decrease in birefringence during the o→h transition was explained in terms of differences in birefringent properties between the orthorhombic and hexagonal structure. Surprisingly, however, the birefringence does not increase very much during cooling (at most 15%), although both X-ray and DSC studies undoubtedly prove the reversibility of the o→h transition. These results imply that the initial drop in birefringence at 151°C (Figure 6) is mainly caused by stress relaxation and partial melting of chain-extended molecules in the rather mobile hexagonal state, giving rise to a decrease in birefringence, rather than by the change in crystal structure itself. Since stress relaxation is an irreversible process, cooling such a sample will not lead to a drastic increase in birefringence. Similar irreversible results were ob-

served for oriented, cross-linked PE tapes, constrained to constant length.⁴² The above results therefore imply small differences in birefringent properties between orthorhombic and hexagonal PE. In literature very little is known about changes in birefringence during similar solid-solid transitions of paraffinoids into the hexagonal phase. Using the paraffin $n\text{-C}_{32}\text{H}_{66}$, West⁴⁴ observed a constancy in birefringence during a temperature induced solid-solid phase transition into a hexagonal structure.

CONCLUDING REMARKS

The o→h transition is a reversible process in case of PE fibres embedded in a matrix. However, due to the increased mobility in the hexagonal phase, partial relaxation/melting occurs. Although improved fibre surface adhesion, optimization of surface/volume ratios and other external variables might increase the constraining efficiency to some extent, the o→h transition occurs within the PE fibres and is consequently difficult to suppress.⁴⁵ In this respect it is of interest to note that constrained chain-extended polypropylene fibres, where a similar solid solid transition is absent, can be heated for prolonged times at for example 200°C (appr. 40°C above the melting point) without a noticeable loss in fibre properties.⁴⁶

Since the o→h solid-solid state transition, is an intrinsic property of PE, the only way to obtain PE fibres which can survive a heat treatment above 155°C is modifying the chemical structure to prevent relaxation. Crosslinking of the fibres is in principle a possibility although the results up to now are not satisfactory.²³ Improvements can be expected in the near future *via* optimization of crosslinking procedures of the PE fibres, adhesion and development of suitable matrices.

Acknowledgements. The authors wish to thank Dr. A. Braam, Dr. P. Froehling, and

Mr. C. Bastiaansen (DSM Research) as well as Dr. G. Ungar (University of Bristol) for fruitful and stimulating discussions. Furthermore they wish to acknowledge Mr. W. Ramaekers (DSM Research) for his valuable technical and experimental support during the performance of the X-ray experiments.

REFERENCES

- J. M. Andrews and I. M. Ward, *J. Mater. Sci.*, **5**, 411 (1970).
- G. Capaccio and I. M. Ward, *Polymer*, **16**, 239 (1975).
- G. Capaccio, T. A. Crompton, and I. M. Ward, *J. Polym. Sci., Polym. Phys. Ed.*, **18**, 301 (1980).
- P. Smith and P. J. Lemstra, *Colloid Polym. Sci.*, **258**, 891 (1980).
- P. J. Lemstra and R. Kirschbaum, *Polymer*, **26**, 1372 (1985).
- P. J. Lemstra, R. Kirschbaum, T. Ohta, and H. Yasuda, "Developments in Oriented Polymers-2," I. M. Ward, Ed., Applied Science Publishers, London, 1987, pp 39-77.
- N. H. Ladizesky and I. M. Ward, *J. Mater. Sci.*, **18**, 533 (1983).
- D. F. Adams, R. S. Zimmerman, and H. W. Chang, *SAMPE J.*, **44** (1985).
- I. M. Ward and N. H. Ladizesky, *Pure Appl. Chem.*, **57**, 1641 (1985).
- N. H. Ladizesky and I. M. Ward, *Comp. Sci. Tech.*, **26**, 129 (1986).
- N. H. Ladizesky, M. Sitepu, and I. M. Ward, *Comp. Sci. Tech.*, **26**, 169 (1986).
- N. H. Ladizesky and I. M. Ward, *Comp. Sci. Tech.*, **26**, 199 (1986).
- P. J. Flory and A. Vrij, *J. Am. Chem. Soc.*, **85**, 3548 (1963).
- A. M. Rijke and L. Mandelkern, *J. Polym. Sci., A-2*, **8**, 225 (1970).
- B. Wunderlich and G. Czornyj, *Macromolecules*, **10**, 906 (1977).
- A. Müller, *Proc. R. Soc. London, Ser. A*, **138**, 514 (1932).
- S. B. Clough, *Polym. Lett.*, **8**, 519 (1970).
- A. J. Pennings and A. Zwijnenburg, *J. Polym. Sci., Polym. Phys. Ed.*, **17**, 1011 (1979).
- J. de Boer, P. F. van Hutten, and A. J. Pennings, *J. Mater. Sci.*, **19**, 428 (1984).
- J. Smook and A. J. Pennings, *Colloid Polym. Sci.*, **262**, 712 (1984).
- R. A. M. Hikmet, Ph. D. Thesis, University of Bristol (1985).
- M. Matsuo and C. Sawatari, *Macromolecules*, **19**, 2028 (1986).
- R. Hikmet, P. J. Lemstra, and A. Keller, *Colloid Polym. Sci.*, **265**, 185 (1987).
- D. C. Bassett, S. Block, and G. J. Piermarini, *J. Appl. Phys.*, **45**, 4146 (1974).
- D. C. Bassett, "Developments in Crystalline Polymers," Vol. 1, D. C. Bassett, Ed., Applied Science Publishers, Essex, England, 1982, Chapter 3.
- M. Yasuniwa, R. Enoshita, and T. Takemura, *Jpn. J. Appl. Phys.*, **15**, 1421 (1976).
- T. Yamamoto, H. Miyaji, and K. Asai, *Rep. Progr. Polym. Phys. Jpn.*, **19**, 191 (1976).
- T. Takemura, *Polym. Prepr. Am. Chem. Soc., Div. Polym. Chem.*, **20**, 270 (1979).
- T. Yamamoto, *J. Macromol. Sci.-Phys.*, **B16**, 487 (1979).
- S. L. Wunder, *Macromolecules*, **14**, 1024 (1981).
- M. Yasuniwa, K. Haraguchi, C. Nakafuku, and S. Hirakawa, *Polym. J.*, **17**, 1209 (1985).
- P. J. Lemstra, N. A. J. M. van Aerle, and C. W. M. Bastiaansen, *Polym. J.*, **19**, 85 (1987).
- P. Smith, P. J. Lemstra, J. P. L. Pijpers, and A. M. Kiel, *Colloid Polym. Sci.*, **259**, 1070 (1981).
- C. W. Bunn and T. C. Alcock, *Trans. Faraday Soc.*, **41**, 317 (1945).
- P. R. Swan, *J. Polym. Sci.*, **56**, 403 (1962).
- G. T. Davis, R. K. Eby, and J. P. Colson, *J. Appl. Phys.*, **41**, 4316 (1970).
- S. Zalwert, *Makromol. Chem.*, **131**, 205 (1970).
- G. A. Jones and H. W. Starkweather, *J. Macromol. Sci.-Phys.*, **B24**, 131 (1985).
- T. Yamamoto, H. Miyaji, and K. Asai, *Jpn. J. Appl. Phys.*, **16**, 1891 (1977).
- T. Asahi, *J. Polym. Sci., Polym. Phys. Ed.*, **22**, 175 (1984).
- T. Kanamoto, T. Hoshiba, T. Yoshimura, K. Tanaka, and M. Takeda, *Rep. Prog. Polym. Phys. Jpn.*, **28**, 227 (1985).
- R. A. M. Hikmet, Personal communications.
- J. C. M. Torfs, Ph. D. Thesis, University of Groningen (1983).
- C. D. West, *J. Am. Chem. Soc.*, **59**, 742 (1937).
- T. Peijs and P. J. Lemstra, to be published.
- C. W. M. Bastiaansen and P. J. Lemstra, submitted to *Polymer*.